Talanta 99 (2012) 865–870

Contents lists available at SciVerse ScienceDirect

Talanta

journal homepage: www.elsevier.com/locate/talanta

High performance of hydrogen peroxide detection using Pt nanoparticles-dispersed carbon electrode prepared by pulsed arc plasma deposition

Takeshi Ito [a,*], Masayuki Kunimatsu [a], Satoru Kaneko [a], Yasuo Hirabayashi [a], Masayasu Soga [a], Yoshiaki Agawa [b], Koji Suzuki [c]

[a] Kanagawa Industrial Technology Center, Shimoimaizumi 705–1, Ebina, Kanagawa 243-0435, Japan
[b] Ulvac-Riko Inc., Hakusan 1-9-19, Midori, Yokohama, Kanagawa 226-0006, Japan
[c] Faculty of Science and Technology, Keio University, Hiyoshi 3-14-1, Kohoku, Yokohama, Kanagawa 223-0061, Japan

ARTICLE INFO

Article history:
Received 31 May 2012
Received in revised form
18 July 2012
Accepted 18 July 2012
Available online 24 July 2012

Keywords:
Pt nanoparticles
Flow injection analysis
Electroanalysis
Arc plasma deposition

ABSTRACT

We propose novel electrodes with platinum nanoparticles dispersed on a glassy carbon (Pt-NPs/GC) prepared using a pulsed arc plasma deposition (APD) method. The method could coat Pt-NPs on a base material directly with a single-step process in a very short deposition time. The characteristics of the electrodes were discussed in detail. The detection of hydrogen peroxide was performed as an example for application of the electrodes. The distribution of nanoparticles was controlled easily by the number of pulse. The surface morphology changed with the pulse number and the annealing except for the sample prepared by 5 pulses deposition (APD(5)), implying that the APD(5) remained as NPs after the annealing. Average particle size was 2.7 nm on the Pt-NPs/GC. Catalyst activity for oxidizing hydrogen peroxide per Pt loading was excellent on the Pt-NPs/GC. When the Pt-NPs/GC was used as a detector for hydrogen peroxide on a flow injection analysis, the Pt-NPs/GC showed high sensitivity without deterioration. Oxidation current increased linearly with the concentration of hydrogen peroxide from 10 nM to 100 μM. This fast and easily prepared electrode showed the capability to replace a conventional bulk metal electrode.

1. Introduction

Metal nanoparticles (NPs) dispersed-electrode is attractive for an electroanalysis because of its high sensitivity. Many methods were introduced to prepare the metal nanoparticles-dispersed electrode, such as implantation [1,2], radio frequency (RF) sputtering [3,4], chemical vapor deposition (CVD) [5–7], polymer supported electrode (PSE) [8–10], and electrochemical deposition (ED) [11–22]. From the viewpoint of the stable supply for users and environmental aspect, a simple fabrication process with easy handling is required with low environmental load. In addition, NPs are required to be coated directly to a base material. The implantation method is not suitable for widespread use because of its high cost of production with difficulty of machine operation and process. The CVD method was introduced to obtain nanoscale Pt clusters by thermolysis of a carbon precursor containing Pt. The method requires polymer synthesis skills and needs waste gas management. Although PSE and ED are simple methods with a cost advantage, these methods need waste liquid treatment, which is at present not suitable with the object of environmental load. RF sputtering and a pulsed arc plasma deposition (APD) method are comparable. However, RF sputtering requires longer process time than the APD method. The sputtering rate is also limited in the narrow range since the deposition rate depends on the type of the material and the sputtering gas. The APD method would satisfy those requirements with easy control of the particle size and dispersion.

The APD method is a physical vapor deposition (PVD) method and attracts attention for preparing nanoparticles and thin film coatings. High grade thin films are obtained by the APD method, because particles generated by the APD method have higher energy than other conventional PVD methods [23]. A wide variety of nanoparticles such as metals, alloys, oxides and even catalytic synthesis of carbon nanotubes have been prepared by this method [24–30]. However, there are no reports describing the characteristics of nanoparticles coated electrode for electroanalysis in detail. Comparing with other conventional PVD methods such as magnetron sputtering and molecular beam epitaxy (MBE), the APD method can control to form nanoparticles to thin film on a substrate by pulse number. Deposition conditions can be varied

* Corresponding author. Tel.: +81 46236 1500; fax: +81 43236 1525.
E-mail address: taito@kanagawa-iri.go.jp (T. Ito).

0039-9140/$ - see front matter © 2012 Elsevier B.V. All rights reserved.
http://dx.doi.org/10.1016/j.talanta.2012.07.048

in a wide range of temperature, deposition pressure, and gas atmosphere, though, the deposition process can become more efficient without temperature and atmosphere control. As a first trial, we tried to coat NPs at room temperature without atmosphere control.

We focused on platinum nanoparticles (Pt-NPs) in this study, because they are used for a wide variety of applications such as medical (e.g. biosensor) [1,3,5–7,11–18], environmental (e.g. gas sensor) [31–34] and energy fields (e.g. proton exchange membrane fuel cell; PEMFC) [35–39]. One example of a biosensing application is a detector for hydrogen peroxide, which is generated by an enzymatic reaction in oxidase-based biosensors. Pt-NPs have a great potential as an electrochemical material to improve the sensitivity of detecting hydrogen peroxide. Many studies have been reported about the performance of Pt-based electrodes and their fabrication method for biosensing [1,3,5–7,11–18]. The surface of the electrode must be flat to decrease the noise level, and highly dispersed Pt-NPs might increase the active area. A carbon electrode coated with Pt-NPs is one of the possible candidates to fulfill these requirements. We report here the characteristics and the electrochemical properties of glassy carbon (GC) electrodes with Pt-NPs prepared using the APD method, and applied the electrodes to detect hydrogen peroxide.

2. Experimental

2.1. Materials

Phosphate buffer solution was prepared to dissolve 67 mM (1/15 M) phosphate buffer powder into distilled water (pH=7.0). The powder, sulfuric acid and hydrogen peroxide were purchased from Wako Pure Chemical Industries, Ltd. (Osaka, Japan). Platinum tablet (3 N) as a target was obtained from Kojundo Chemical Laboratory Co., Ltd. (Saitama, Japan). GC substrate (10 mm × 10 mm × 0.5 mm thick) was used as an electrode substrate and purchased from Tokai Carbon Co., Ltd. (Tokyo, Japan).

2.2. Nanoparticle coating

The GC substrate was exposed to Ar plasma for 60 sec with the plasma energy of 35 W (GD-OES, Horiba, Japan) before Pt-NPs coating. The APD system (APD-P, Ulvac-Riko Inc., Japan) was used to prepare Pt-NPs with an applied voltage of 150 V and a capacitor capacitance of 1080 μF. The system did not employ DC cathodic arc sources but a pulsed arc source. The distance between the target and the substrate was set to 140 mm. Pt metal was deposited at room temperature with the operating frequency of 1 Hz at a pressure of 5×10^{-3} Pa. We only changed the pulse number on the deposition from 5 to 20 (deposition time: 5 s–20 s). For simplification, we refer to the sample condition as APD(pulse number). After the deposition, GC electrodes coated with Pt-NPs were annealed at 200 °C for 30 min with N_2 gas including 0.25 vol% H_2 gas.

2.3. Instrumentation and measurements

X–ray photoelectron spectroscopy (XPS) (Model 5500, Ulvac-Phi, Inc., Japan) was employed to estimate a quantitative composition of the electrodes. The surface roughness was measured by an atomic force microscopy (AFM) (SPI 3800, SII Nano Technology Inc., Japan) with the tapping mode in air using a SI-DF40 cantilever. Horizontal dispersion of Pt-NPs was monitored by field emission type transmission electron microscopy (FE-TEM) (EM002BF, Topcon Technohouse Co., Japan) with a high-angle annular dark-field (HAADF) mode.

2.4. Electrochemical measurements and flow injection analysis

Electrochemical properties of the GC electrodes with Pt-NPs were evaluated by using a potentiostat (ALS832, CH Instrument, USA) with a plate material evaluating cell (BAS Co., Ltd., Japan) consisting of the prepared electrode as a working electrode (WE, active area=0.11 cm^2), a reference electrode (RE) and a Pt wire counter electrode (CE). Reversible hydrogen electrode (RHE) and Ag/AgCl (3 M NaCl) electrode were used for the RE in 0.5 M sulfuric acid solution and in the phosphate buffer solution, respectively.

We set the prepared electrode in a flow injection analysis (FIA) system as an electrochemical detector. A radial flow cell (BAS Co. Ltd., Japan) was used for the detector consisting of the prepared electrode for WE, an Ag/AgCl electrode for RE, and a stainless electrode for CE. Active area of the electrode was defined as 0.6 cm^2 with a 25 μm thick spacer. The phosphate buffer solution was used as a carrier solution. A microsyringe pump (CMA-102, CMA Microdialysis, Sweden) induced the carrier solution from a microsyringe (1 mL, Hamilton, USA) to the flow cell through a 6-port injection valve (V-485-DC, Upchurch Scientific, USA). Hydrogen peroxide was dissolved into the phosphate buffer solution from 10 nM to 1 mM. Sample loop had 1 μL volume, and the dead volume of the injection valve was 35 nL. The capillary tube obtained from Upchurch Scientific had outside and inside diameters of 360 and 100 μm, respectively. After the prepared electrode was set in the flow cell and connected to the potentiostat, amperometric detection was carried out. All the measurements were carried out at room temperature.

3. Results and discussion

3.1. Nanoparticle characterization

The APD method is known as a coating technology with great potential, because the arc plasma is fully ionized and manipulated with electric and magnetic fields. Ion energy affects the structure and property of the film, and is influenced by the electric field. Magnetic field is commonly used to guide and homogenize the plasma. The kinetic energy of Pt on the APD method was estimated as 67 eV [40]. The kinetic energy indicated that Pt-NPs had good adhesion to a substrate. The results of differential scanning calorimetry (DSC) analysis showed that Pt loading increased with the pulse number linearly. Pt loading rate on our deposition condition showed the constant of 2.08 μg/cm^2/pulse, indicating that the APD method could control the Pt loading precisely.

Before the GC substrate was sputtered by Ar plasma, the surface had polishing flaws with a surface roughness (average roughness=Ra) of 1.91 nm. AFM images scanned over 1 μm × 1 μm with the tapping mode showed quite a flat surface with Ra of 0.53 nm after the Ar sputtering. The Ar sputtering was effective for planarization even with very short time (only 60 s). The GC electrodes with Pt-NPs also had quite flat surfaces after the deposition (Ra=0.55–0.65).

HAADF-STEM images of APD(5–20) before and after the annealing are presented in Fig. 1(a). On the APD(5), Pt-NPs (bright spots) were well dispersed. Fig. 1(b) shows a high resolution FE-TEM image after annealing the APD(5). The distribution of the metal particle size was narrow with an average size of 2.7 nm. Particle size and distribution were nearly unchanged after the annealing. By contrast, small islands consisting of very small particles were found on the APD(10). After the annealing, the particles disappeared and formed islands. Even after 20 s deposition, Pt thin film did not cover the entire surface of the APD(20),

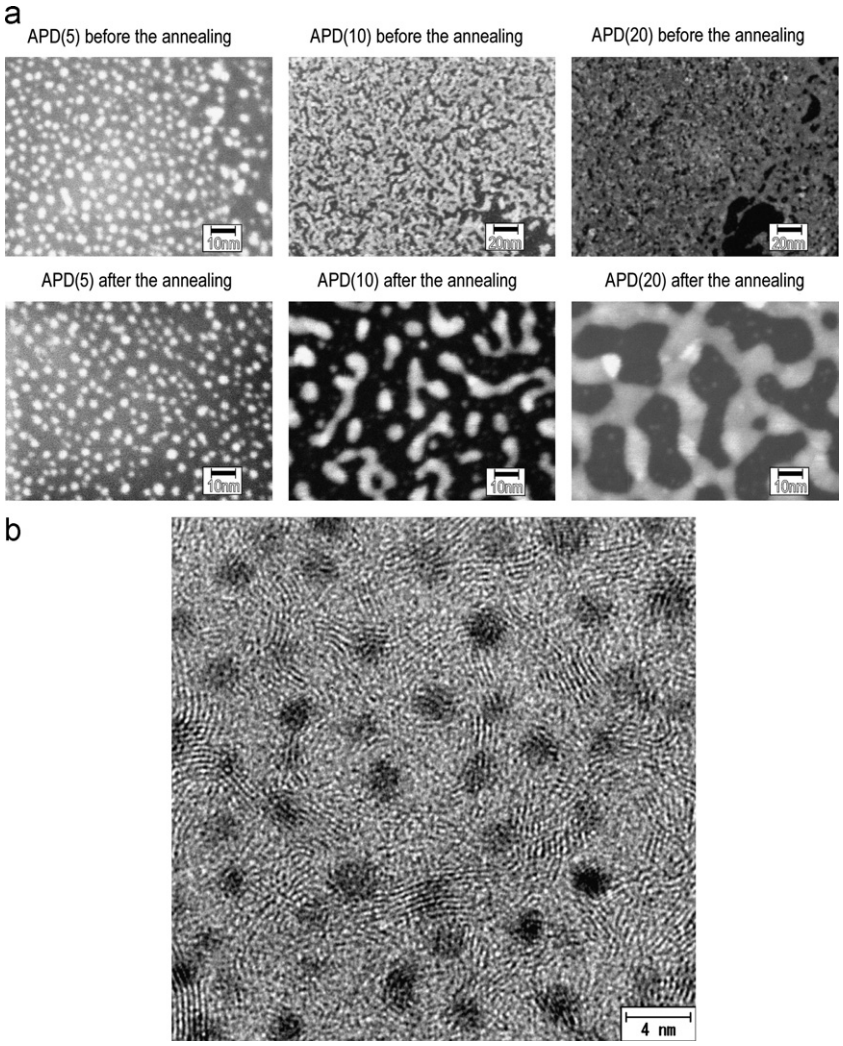

Fig. 1. (a) HAADF-STEM images of APD(5–20) before and after the annealing. (b) High resolution FE-TEM image of APD(5) after the annealing.

and network of Pt nano-structure appeared after the annealing. These results showed that APD(5) was the only Pt-NPs dispersed GC electrode (Pt-NPs/GC), and the APD method could produce Pt-NPs in a short time without temperature and atmosphere control, which is superior to other PVD methods. Pulsed laser deposition (PLD) needs over 60 s to increase the density of Pt-NPs, which made some cluster formation [41]. Atmosphere control is necessary when using the sputtering method. In addition, sputtering rate is dependent on the target material and induced gas.

XPS was used to estimate the quantitative composition of the electrodes. In order to estimate the binding energy of Pt(4f), C(1s) was used as an internal reference (284.5 eV). The atomic concentration of Pt increased with the pulse number. High resolution XPS spectra of Pt(4f) line of APD(5–20) and APD(5, 10) after the annealing are plotted on Fig. 2. The binding energies of the Pt($^4f_{7/2}$) and Pt($^4f_{5/2}$) electrons increased with decreasing pulse number. Peak separations of each spectrum were 3.3 eV, which was equal to that on bulk Pt. The binding energy of Pt($^4f_{7/2}$) electrons on the APD(5), APD(10) and APD(20) were 72.1 eV, 71.6 eV and 71.6 eV, respectively. The binding energy of the APD(5) was 0.9 eV higher than that of bulk polycrystalline Pt (71.2 eV). After the annealing, the binding energy on the APD(5) and APD(10) decreased to 71.4 eV and 71.3 eV, respectively. The positive shift of the binding energy of Pt($^4f_{7/2}$) electron against bulk Pt was due to the size effect of small particles [42]. After the annealing, the amount of positive shift decreased on all the samples. The decrease of positive shift on the APD(10) after the annealing was mainly due to the drastic change of morphology. However, shape of Pt-NPs did not change on the APD(5) after the annealing. In this case, the decrease of positive shift might be caused by removal of adsorbed impurities. These results indicated that the Pt-NPs existed in the Pt(0) state.

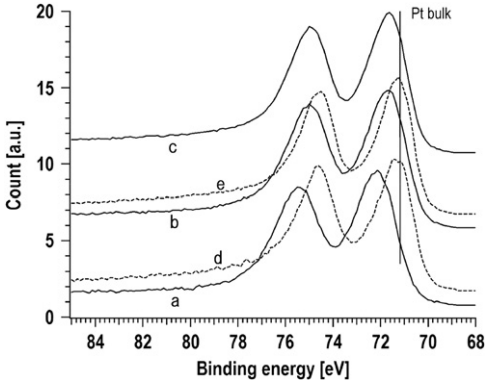

Fig. 2. High resolution XPS spectra of Pt(4f) line on the APD samples of (a) APD(5), (b) APD(10), and (c) APD(20) before the annealing. (d) and (e) show the spectra after the annealing on the APD(5) and APD(10), respectively. Pt($^4f_{7/2}$) on bulk was inserted in spectra.

3.2. Electrochemical properties

Cyclic voltammograms (CVs) of APD(5–20) before and after the annealing were measured in 0.5 M sulfuric acid solution bubbling with N_2 gas as shown in Fig. 3. Since electrochemical (EC) cleaning over 1.0 V vs. RHE caused the change of crystalline surface structure [43]; we cleaned the electrodes by scanning from 0.05 to 0.8 V for 100 cycles with the sweep rate of 100 mV/s before evaluating the CVs with the sweep rate of 50 mV/s. Before the annealing, CVs of APD(5–20) had no peaks corresponding to the crystal orientation of Pt in the lower potential range, representing the reduction of absorbed hydrogen and the formation of absorbed hydrogen. This result showed that impurity adsorption on the surface of Pt-NPs was not decontaminated completely by such a mild EC cleaning. Current density increased with the pulse number independently of the annealing, which affected Pt loading as discussed above. The annealed electrodes progressed in current density, and peaks appeared at the lower potential range. The result indicated that the annealing in H_2 gas was effective to remove impurities. The effective Pt surface area (A_{Pt}) was calculated using the following equation:

$$A_{Pt}[cm^2] = \int i \times dt / Q_{Pt0},$$

where i, dt and Q_{Pt0} are current, time, and theoretical charge amount per unit area of bulk Pt (210 μC/cm^2), respectively. As shown in Table 1, the effective Pt surface area, A_{Pt}, increased after the annealing on each sample since the surface was cleaned at high temperature with H_2 gas.

3.3. Hydrogen peroxide detection

Hydrogen peroxide is one of the important substances for detecting bio-materials, since there are many oxidase-based biosensors. Additionally, a highly sensitive detection of hydrogen peroxide is anticipated since it is known as a stress marker [44,45]. We observed CVs of the GC electrode and APD(5–20) in the phosphate buffer solution including 1 mM hydrogen peroxide. The potential of the WE was scanned from 0.2 to 0.8 V vs. Ag/AgCl with the sweep rate of 50 mV/s. For example, Fig. 4(a) shows CVs of the GC electrode and APD(5) before and after the annealing. The GC electrode did not show any significant oxidation peaks, indicating low detection sensitivity for hydrogen peroxide in this potential range. By contrast, CVs on each APD(5) had the oxidation peak. Magnitude of the oxidation peak increased after the annealing. Fig. 4(b) shows the current density at the oxidation peak and catalyst activity for hydrogen peroxide corresponding to the pulse number on the prepared electrode before and after the annealing. The catalyst activity, CA, was calculated as given below:

CA=current at the oxidation peak [mA]/electrode area [cm^2]/Pt loading [μg].

The CA decreased with increasing pulse number, and the APD(5) after the annealing showed the highest CA in our experiments. Current density at the oxidation peak decreased gradually over 10 pulses. The electrodes showed high activity after the annealing since impurities were removed, and the morphology of deposited material was changed. The potential at the oxidation

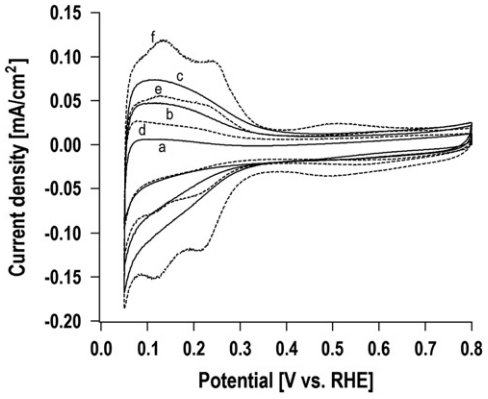

Fig. 3. Cyclic voltammograms in 0.5 M sulfuric acid solution on the APD samples of (a) APD(5), (b) APD(10), and (c) APD(20) before the annealing. (d), (e) and (f) show CVs after the annealing on the APD(5), APD(10) and APD(20), respectively. The potential of the WE was scanned from 0.05 to 0.8 V vs. RHE with a sweep rate of 50 mV/s.

Table 1
The real surface area of Pt (A_{Pt}) was estimated from the charge corresponding to the hydrogen reduction and the hydrogen absorption in Fig. 3.

Sample	Before the annealing A_{Pt} (cm^2)	After the annealing A_{Pt} (cm^2)
APD(5)	0.03	0.04
APD(10)	0.09	0.1
APD(20)	0.17	0.23

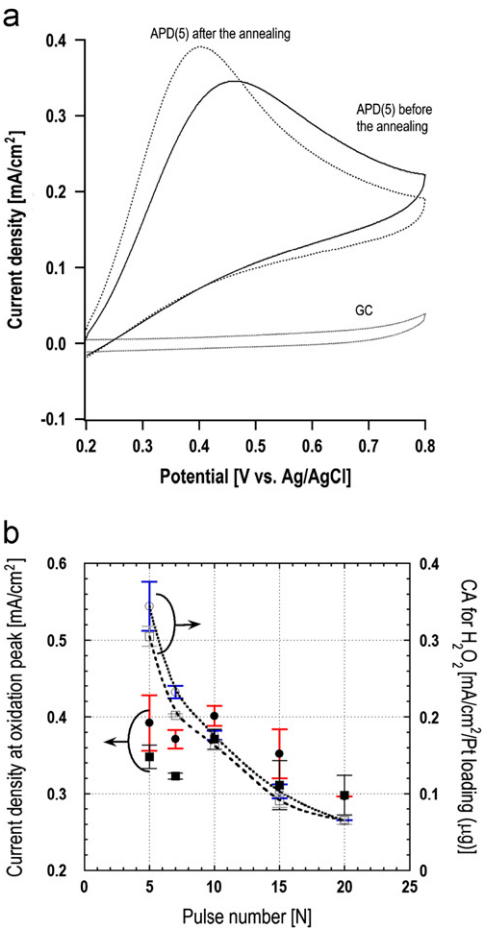

Fig. 4. (a) Cyclic voltammograms of the GC and APD(5) before and after the annealing in 1/15 M phosphate buffer solution (pH=7.0) including 1 mM hydrogen peroxide. The potential of the WE was scanned from 0.2 to 0.8 Vvs. Ag/AgCl with the sweep rate of 50 mV/s. (b) Current density at oxidation peak and catalytic activity (CA) for hydrogen peroxide were plotted against the pulse number. Squares and circles show the electrode conditions before and after the annealing, respectively. CA was calculated as oxidation peak current/electrode area/Pt loading. These data were obtained from CVs in phosphate buffer solution with 1 mM hydrogen peroxide.

peak on the APD(5) after the annealing was about 0.4 V vs. Ag/AgCl. The APD(5) was in optimal condition to be used for an electrode with high sensitivity for hydrogen peroxide since the APD(5) was the only Pt-NPs/GC. The stability of the APD(5) without the annealing was examined on CV in PBS containing 1 mM H_2O_2. After the first evaluation, the sample was left atmospherically exposed for 16 months at room temperature. Current at oxidation peak on the 16-month-old sample was almost the same as the result of the first evaluation. This result indicated that performance degradation was not observed on the APD(5) without the annealing.

Penner and co-workers revealed the condition to control the size and dispersion of Pt-NPs by ED [19–22]. However, there were not many reports discussing the catalytic performance per Pt loading on hydrogen peroxide detection using ED. Chikae et al. reported the direct coating of Pt-NPs on screen-printed carbon electrode [18]. The distribution of particle size was scattered from 80 to 130 nm. The potential and current density at the oxidation peak for hydrogen peroxide were about 0.6 Vvs. Ag/AgCl and 0.3 mA/cm^2, respectively. By contrast, RF sputtering could supply 2.5 nm Pt-NPs embedded in carbon film [3]. The potential and current density at the oxidation peak for hydrogen peroxide were about 0.5 Vvs. Ag/AgCl and 0.35 mA/cm^2, respectively. Comparing with those reports, our Pt-NPs/GC had excellent catalytic activity on potential (0.4 Vvs. Ag/AgCl) and current density (0.39 mA/cm^2) at the oxidation peak.

Pt-NPs/GC was applied into the detector of the FIA system. The WE potential was set to 0.4 Vvs. the RE to oxidize hydrogen peroxide. The flow rate ranged from 5 to 15 μL/min. Height of the current peak and peak area were determined as *Ip* and *Q*, respectively. Electric charge *Q* shows the amount of hydrogen peroxide oxidized on the electrode, and was calculated as an integration of current at the current peak. Although *Ip* increased with the flow rate, *Q* had a peak around the flow rate of 7.5 μL/min. It takes longer to determine the period with lower flow rate. Judging from the measuring time and the magnitude of the responses, a calibration curve was obtained both on *Ip* and *Q* at the flow rate of 10 μL/min. Examples of the response on FIA were shown in Fig. 5. Current increase was recognized even in 10 nM. Noise around 10 s, 40 s and 70 s were caused by valve operation in the FIA system. The time from sample injection to peak end was within 30 s. The efficiency of electrochemical reaction was estimated at the detector as a trap ratio. The trap ratio can be expressed as

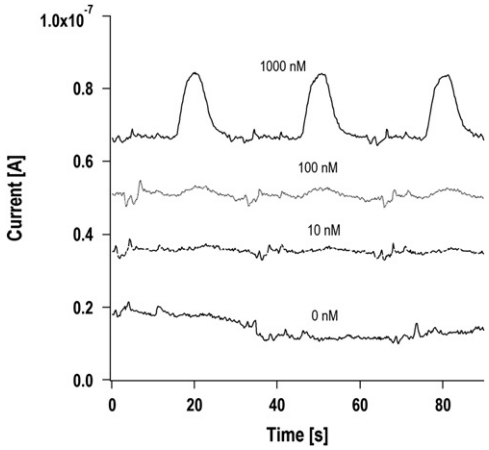

Fig. 5. Examples of FIA response on the Pt-NPs/GC with various concentration of hydrogen peroxide (0–1000 nM). The flow rate was 10 μL/min. The WE potential was set to 0.4 V vs. RE (Ag/AgCl). Each data were offset in current direction.

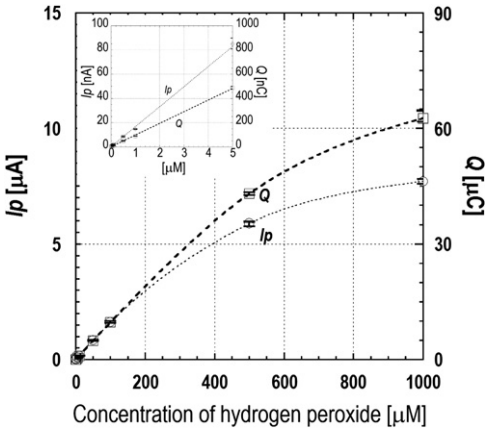

Fig. 6. Calibration curve using *Ip* and *Q* for hydrogen peroxide at the condition of Fig. 5. Calibration curve at lower range (10 nM–5 μM) is included on the upper left corner. Open circles and squares show *Ip* and *Q*, respectively.

trap ratio [%]=measured *Q*/theoretical electric charge (9.65×10^{-6}C, 1 μL injection of 100 μM hydrogen peroxide) × 100.

The trap ratio of hydrogen peroxide at the flow rate of 10 μL/min was expected as 97.6%, which indicated that our FIA system worked well. *Ip* and *Q* were measured with hydrogen peroxide concentration from 10 nM to 1 mM by five times measurements at each concentration. The responses of *Ip* and *Q* against hydrogen peroxide concentration showed linear relation in the range from 10 nM to 100 μM with correlation coefficients of 0.9998 and 0.9999, respectively, as shown in Fig. 6. The detection limit (S/N=3) was 13.5 nM, which indicated that the system could detect 13.5 fmol of hydrogen peroxide. These results showed that our FIA system had high sensitivity with low sample volume and short detection time. We studied the response dependent on repetition of sample injections for 100 times to evaluate the durability of the electrode. As a result, the electrode response was stable among the experiments. Coefficient of variation (CV) was 4.8%.

4. Conclusion

GC electrodes coated with Pt-NPs by the pulsed APD method were demonstrated to be a superior electrode for detecting hydrogen peroxide. The APD method can supply nanoparticles with fine particle size and narrow size distribution with 5 pulses (APD(5)). Surface morphology was dependent on the pulse number and annealing process, except for the APD(5); morphology on the APD(5) was unchanged after the annealing. Only the APD(5) formed Pt-NPs on the GC substrate. Catalyst activity for hydrogen peroxide per Pt loading showed the best performance on the Pt-NPs/GC in this study. As the results of applying the Pt-NPs/GC for the detector on the FIA system, the electrode had good durability and repeatability with low detection limit. These results indicated that the APD method can supply the functional electrode superior to conventional bulk metal electrodes.

Acknowledgments

We thank Mr. S. Konuma of the Kanagawa Academy of Science and Technology for discussion of the TEM analysis and Dr. D. Citterio of Keio University for discussion of the properties of the electrode. This work was supported by The Ministry of Education, Culture, Sports, Science and Technology (MEXT), Japan (Grant in Aid for Young Scientist (B), no. 21710134).

References

[1] T.A. Ivandini, R. Sato, Y. Makide, A. Fujishima, Y. Einaga, Chem. Lett. 33 (2004) 1330.
[2] R. Uchikado, T.N. Rao, D.A. Tryk, A. Fujishima, Chem. Lett. 30 (2001) 144.
[3] T. You, O. Niwa, M. Tomita, S. Hirono, Anal. Chem. 75 (2003) 2080.
[4] T. You, O. Niwa, Z. Chen, K. Hayashi, M. Tomita, S. Hirono, Anal. Chem. 75 (2003) 5191.
[5] M.R. Callstrom, T.X. Neeman, R.L. McCreery, D.C. Alsmeyer, J. Am. Chem. Soc. 112 (1990) 4954.
[6] N.L. Pochard, D.C. Alsmeyer, R.L. McCreery, T.X. Neenan, M.R. Callstrom, J. Matter. Chem. 2 (1992) 771.
[7] N.L. Pochard, D.C. Alsmeyer, R.L. McCreery, T.X. Neenan, M.R. Callstrom, J. Am. Chem. Soc. 114 (1992) 769.
[8] P. Karam, L.I. Halaoui, Anal. Chem. 80 (2008) 5441.
[9] D.K. Park, S.J. Lee, J-H. Lee, M.Y. Choi, S.W. Han, Chem. Phys. Lett. 484 (2010) 254.
[10] M-J. Song, J.H. Kim, S.K. Lee, H-H. Lee, D.S. Lim, S.W. Hwang, D. Whang, Microchim Acta 171 (2010) 249.
[11] O. Niwa, T. Horiuchi, M. Morita, T. Huang, T. Kissinger, Anal. Chim. Acta 318 (1996) 167.
[12] A. Kicela, S. Daniel, Talanta 68 (2005) 1632.
[13] J. Wang, N.V. Myung, M. Yun, H.G. Monbouquette, J. Electroanal. Chem. 575 (2005) 139.
[14] G.F. Khan, W. Wernet, Anal. Chim. Acta 351 (1997) 151.
[15] D.E. Weisshaar, T. Kuwana, J. Electroanal. Chem. 163 (1984) 395.
[16] H-K. Seo, O-J. Park, J-Y. Park, Thin Solid Films 516 (2008) 5227.
[17] H. Xu, L. Zeng, S. Xing, G. Shi, J. Chen, Y. Xian, L. Jin, Electrochem. Commun. 10 (2008) 1893.
[18] M. Chikae, K. Idegami, K. Kerman, N. Nagatomi, M. Ishikawa, Y. Takamura, E. Tamiya, Electrochem. Commun. 8 (2006) 1375.
[19] J.V. Zoval, J. Lee, S. Gorer, R.M. Penner, J. Phys. Chem. B 102 (1998) 1166.
[20] J.L. Fransaer, R.M. Penner, J. Phys. Chem. B 103 (1999) 7643.
[21] H. Liu, R.M. Penner, J. Phys. Chem. B 104 (2000) 9131.
[22] R.M. Penner, J. Phys. Chem. B 105 (1999) 8672.
[23] A. Anders, E. Oks, J. Appl. Phys. 101 (2007) 043304.
[24] S. Hinokuma, K. Murakami, K. Uemura, M. Matsuda, K. Ikeue, N. Tsukahara, M. Machida, Top. Catal. 52 (2009) 2108.
[25] T. Fujitani, I. Nakamura, T. Akita, M. Okumura, M. Haruta, Angew. Chem. Int. Ed. 48 (2009) 9515.
[26] F.S. Teixeira, M.C. Salvadori, M. Cattani, S.M. Carneiro, I.G. Brown, J. Vac. Sci. Technol. B 27 (2009) 2242.
[27] Z. Wei, P. Yan, W. Feng, J. Dai, T. Xia, Mater. Charact. 57 (2006) 176.
[28] M.Z. Shoushtari, S. Parhoodeh, M. Farbod, J. Physics: Conf. Series 100 (2008) 052017.
[29] J. Chen, G. Lu, Nanotechnology 17 (2006) 2891.
[30] D. Phokharatkul, Y. Ohno, H. Nakano, S. Kishimoto, T. Mizutani, Appl. Phys. Lett. 93 (2008) 053112.
[31] R. Dolbec, M.A.EI Khakani, Appl. Phys. Lett. 90 (2007) 173114.
[32] M. Gaidi, B. Chenevier, M. Labeau, Sens. Actu. B 62 (2000) 4.
[33] X. Xue, Z. Chen, C. Ma, L. Xing, Y. Chen, Y. Wang, J. Phys. Chem. C 114 (2010) 3968.
[34] W. Wongwiriyapan, S. Inoue, T. Ito, R. Shimazaki, T. Maekawa, K. Suzuki, H. Ishikawa, S. Honda, K. Oura, M. Katayama, Appl. Phys. Express 1 (2008) 014004.
[35] K.A. Starz, E. Auer, T. Lehmann, R. Zuber, J. Power Sources 84 (1999) 167.
[36] K.B. Prater, J. Power Sources 37 (1992) 181.
[37] B.C.H. Steele, A. Heinzel, Nature 414 (2001) 345.
[38] C. Bernay, M. Marchand, M. Cassir, J. Power Sources 108 (2002) 139.
[39] E.J. Taylor, E.B. Anderson, N.R.K. Vilambi, J. Electrochem. Soc. 139 (1992) L45.
[40] A. Anders, Vacuum 67 (2002) 673.
[41] T. Ito, S. Kaneko, M. Kunimatsu, Y. Hirabayashi, M. Soga, K. Suzuki, Int. J. Electrochem. 2011 (2011) 463281.
[42] T.T.P. Cheung, Surf. Sci. 140 (1984) 151.
[43] J. Solla–Gullón, V. Montiel, A. Aldaz, J. Clavilier, J. Electroanal. Chem. 491 (2000) 69.
[44] E.W. Miller, C.J. Chang, Curr. Opin. Chem. Biol. 11 (2007) 620.
[45] P.N. Dekhuijzen, K.K. Aben, I. Dekker, L.P. Aarts, Am. J. Respir. Crit. Care Med. 154 (1996) 813.